Journal of Organometallic Chemistry 696 (2011) 2772–2781

Contents lists available at ScienceDirect

Journal of Organometallic Chemistry

journal homepage: www.elsevier.com/locate/jorganchem

New dimeric and supramolecular organotin(IV) complexes with a tridentate schiff base as potential biocidal agents

Shaukat Shujah [a], Zia-ur-Rehman [a], Niaz Muhammad [a], Saqib Ali [a,*], Nasir Khalid [b], Muhammad Nawaz Tahir [c]

[a] Department of Chemistry, Quaid-i-Azam University, Islamabad 45320, Pakistan
[b] Chemistry Division, Pakistan Institute of Nuclear Science and Technology, PO Nilore, Islamabad, Pakistan
[c] University of Sargodha, Department of Physics, Sargodha, Pakistan

ARTICLE INFO

Article history:
Received 8 March 2011
Received in revised form
6 April 2011
Accepted 11 April 2011

Keywords:
Organotin(IV) derivatives
ONO schiff base
Dimeric
Supramolecular
Antifungal
Antibacterial
Antileishmanial
Antiurease

ABSTRACT

The paper describes the synthesis and structural characterization of six new diorganotin(IV) compounds 1–6, [R_2SnL] and a monoorganotin(IV) derivative, C_4H_9SnClL (7). Here L = N′-(5-bromo-2-oxidobenzylidene)-N-(oxidomethylene)hydrazine ligand with ONO tridentate chelation capability and R = CH_3 (**1**), C_2H_5 (**2**), n-C_4H_9 (**3**), C_6H_5 (**4**), C_8H_{17} (**5**), $tert$-C_4H_9 (**6**), The packing diagram offers a supramolecular structure for **1** and a dimeric structure for **4** with distorted square-pyramidal and distorted trigonal geometry, respectively. The different geometry of **1** than **4** can be attributed to the presence of intermolecular non-covalent Sn—O and Sn—H interactions in the former. The antifungal, antibacterial, antiurease and antileishmanial activities of these complexes proved them to be active biologically and may be formulated as new metal-based drugs in future.

1. Introduction

Schiff base ligands received instant and enduring popularity not only they have played a seminal role in the development of modern coordination chemistry [1], but they can also be found at key points in the development of inorganic chemistry [2], catalysis [3,4] medicinal imaging [5], optical materials [6], and thin films [7,8]. The chemistry of organotin(IV) has been the area of interest for many years because of their industrial and biomedical applications [9]. Several organotin(IV) complexes have been found as affective antifouling [10], anti-microbial [11] and antiviral agents. Organotin(IV) complexes with schiff base ligands have been an area of focus owing to their anti-tumor activities [12–20]. In addition to this, the complexes belonging to this class also present interesting structural diversities [21]. Keeping in view all these points and as an extension of our previous work, we synthesized and characterized seven new organotin(IV) derivatives of a ONO tridentate schiff base, N′-(5-bromo-2-oxidobenzylidene)-N-(oxidomethylene)hydrazine, and carried out their antifungal, antibacterial, antiurease and antileishmanial activities. This paper is unique in the sense that the antiurease and antileishmanial activities for organotin(IV) schiff bases are scantly available in the literature and the given article may be the first step in this direction. The profound antileishmanial activities demand further investigations on these complexes to be used as antileishmanial agents in future.

2. Experimental

2.1. Chemicals

Organotin(IV) dichlorides, dioctyltin(IV) oxide, butyltin(IV) chloridedihydroxide, 5-bromo-2-hydroxybenzaldehyde and formic hydrazide were procured from Aldrich. The organic solvents (toluene, chloroform, hexane, ethanol etc.) were used of Merck, Germany and were dried *in situ* using standard procedures [22] and freshly collected prior to use.

2.2. Instrumentation

The melting points were determined on an electrothermal melting point apparatus, model MP-D Mitamura Rieken Kogyo

* Corresponding author. Tel.: +92 51 90642130; fax: +92 51 90642241.
E-mail address: drsa54@yahoo.com (S. Ali).

0022-328X/$ – see front matter © 2011 Elsevier B.V. All rights reserved.
doi:10.1016/j.jorganchem.2011.04.010

(Japan) by using capillary tubes and are uncorrected. The infrared (IR) spectra were recorded as neat liquids, using NaCl cells or as KBr pellets for solids on a Bio-Rad Excaliber FT-IR, model FTS 300 MX spectrophotometer (USA) in the frequency range of 4000–400 cm^{-1}. Multinuclear NMR (^1H, ^{13}C, and ^{119}Sn) spectra were recorded on a Bruker ARX 300 MHz-FT-NMR and a Bruker 400 MHz-FT-NMR spectrometers Switzerland using $CDCl_3$ as an internal reference. Chemical shifts (δ) are given in ppm and coupling constants (J) are given in Hz. The multiplicities of signals in ^1H NMR are given with chemical shifts; (s = singlet, d = doublet, t = triplet, q = quartet, m = multiplet).

The mass spectra were recorded on a MAT-311A Finnigan (Germany). The m/z values were evaluated assuming that H = 1, C = 12, N = 14, O = 16, Cl = 35 and Sn = 120. The X-ray diffraction data were collected on a Bruker SMART APEX CCD diffractometer, equipped with a 4 K CCD detector set 60.0 mm from the crystal. The crystals were cooled to 100 ± 1 K using the Bruker KRYOFLEX low-temperature device and Intensity measurements were performed using graphite monochromated Mo-Kα radiation from a sealed ceramic diffraction tube (SIEMENS). Generator settings were 50 kV/40 mA. The structure was solved by Patterson methods and extension of the model was accomplished by direct methods using the program *DIRDIF* or SIR2004. Final refinement on F^2 carried out by full-matrix least squares techniques using SHELXL-97, a modified version of the program *PLUTO* (preparation of illustrations) and *PLATON* package.

2.3. Syntheses

2.3.1. Synthesis of N′-(5-bromo-2-hydroxybenzylidene)formohydrazide (H_2L)

An ethanolic solution of 5-bromo-2-hydroxybenzaldehyde 3.35 g (16.65 mmol) was added slowly to the solution of formic hydrazide 1.0 g (16.65 mmol), in ethanol with constant stirring at room temperature. The mixture was refluxed for 1 h and on cooling yellow crystalline solid was obtained (Scheme 1a). m.p. 256–258 °C. Yield 80% (3.236 g). *Anal.* Calc. for $C_8H_7BrN_2O_2$ (M = 242): C, 39.53; H, 2.90; N, 11.53 Found: C, 39.50; H, 2.89; N, 11.57%. IR (cm^{-1}): 1706 ν(C=O), 3185 ν(NH), 1098 ν(N–N), 1609 ν(C=N), 3410 ν(OH)$_{Phenolic}$.

2.3.2. Synthesis of Dimethyltin(IV) [N′-(5-bromo-2-oxidobenzylidene)-N-(oxidomethylene)hydrazine]; (**1**)

A 250 mL two-necked flask containing 100 mL toluene, equipped with a reflux condenser was charged with N′-(5-bromo-2-hydroxybenzylidene)formohydrazide 0.73 g (3.0 mmol), and triethylamine 0.84 mL (6.0 mmol) along with a magnetic bar. To the solution of triethylammonium salt of the ligand, dimethytin(IV) dichloride (0.66 g, 3.0 mmol) in dry toluene was added drop wise into the flask with stirring at room temperature. The solution turned yellow, it was stirred for 5 h at room temperature. The white precipitates of Et_3NHCl formed during the reaction were filtered. The filtrate was concentrated by rotary evaporator to obtain yellow solid. The product was recrystallized from $CHCl_3$/n-hexane (4:1) mixture (Scheme 1b).

IR(cm^{-1}): 1609 ν(C=N), 1079 ν(N–N), 566 ν(Sn–O), 498 ν(Sn–N)

2.3.3. Diethyltin(IV) [N′-(5-bromo-2-oxidobenzylidene)-N-(oxidomethylene)hydrazine]; (**2**)

Compound 2 was prepared in the same way as **1**, using following quantities: N′-(5-bromo-2-hydroxybenzylidene)formohydrazide 0.73 g (3.0 mmol), diethyltin(IV) dichloride 0.74 g (3.0 mmol), triethylamine 0.84 mL (6.0 mmol) were reacted in 1:1:2 ratio. Solid product was recrystallized in chloroform and n-hexane (4:1) mixture. IR (cm^{-1}): 1605 ν(C=N), 1080 ν(N–N), 563 ν(Sn–O), 488 ν(Sn–N).

2.3.4. Dibutyltin(IV) [N′-(5-bromo-2-oxidobenzylidene)-N-(oxidomethylene)hydrazine]; (**3**)

Compound **3** was prepared in the same way as **1**, using following quantities: N′-(5-bromo-2-hydroxybenzylidene)formohydrazide 0.73 g (3.0 mmol), dibutyltin(IV) dichloride 0.91 g (3.0 mmol), triethylamine 0.84 mL (6.0 mmol) were reacted in 1:1:2 ratio. Viscous liquid product was obtained. IR (cm^{-1}): 1625 ν(C=N), 1088 ν(N–N), 548 ν(Sn–O), 472 ν(Sn–N).

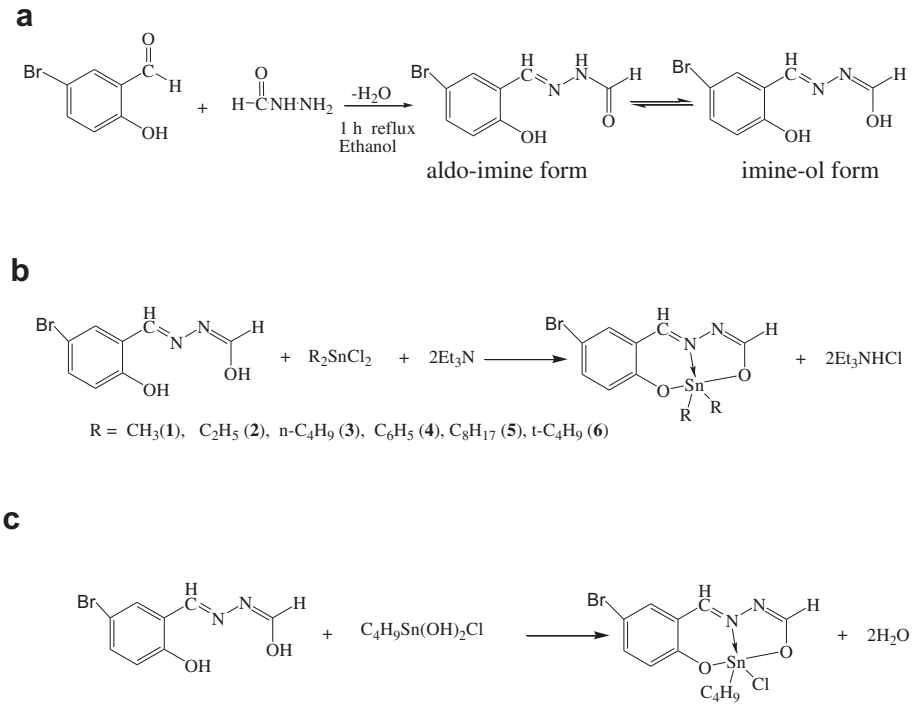

Scheme 1. Synthesis of N′-(5-bromo-2-hydroxybenzylidene)formohydrazide (H_2L) *(a), diorganotin(IV) derivatives (b) and* butylchloridetin(IV) derivative (c).

Table 1
^{1}H NMR data of N′-(5-bromo-2-hydroxybenzylidene)formohydrazide (H_2L)[a,b,c] and its organotin(IV) derivatives.

Proton		Chemical Shift (ppm)						
	H_2L	(1) Me_2SnL	(2) Et_2SnL	(3) n-Bu_2SnL	(4) Ph_2SnL	(5) Oct_2SnL	(6) ter-Bu_2SnL	(7) BuClSnL
–CH=N–	8.26 (s)	8.53 (s) [44]	8.55 (s) [41]	8.52 (s) [40]	8.56 (s) [48]	8.51 (s) [40]	8.55 (s) [37]	8.72 (s)
–N=CHO–	–	7.64 (s)	7.69 (s)	7.66 (s)	7.89 (s)	7.66 (s)	7.75 (s)	7.76 (s)
Br (ring)	6.86 (d, 8.7)	6.66 (d, 9.0)	6.68 (d, 9.0)	6.65 (d, 9.0)	7.01 (d, 9.0)	6.64 (d, 9.0)	6.72 (d, 9.0)	6.79 (d, 9.0)
	7.37	7.39	7.38	7.36	7.45–7.52	7.35	7.37	7.47
	(dd, 2.7, 8.7)	(dd, 2.7, 9.0)	(dd, 2.7, 9.0)	(dd, 2.7, 9.0)	(m) 7.30 (s)	(dd, 2.7, 9.0)	(dd, 2.7, 9.0)	(dd, 2.4, 9.0)
	7.75 (s)	7.25 (s)	7.26 (s)	7.24 (s)		7.24 (s)	7.24 (s)	7.25 (s)
R α	–	0.83 (s) [76, 79]	1.49 (m)	1.57–1.65 (m)	–	1.60–1.67 (m)	–	1.66–1.75 (m)
β	–	–	1.29 (*t*, 7.5)	1.47–1.51 (m)	7.81–7.84 (m)	1.47–1.52 (m)	1.32(s) [107, 112]	1.52–1.58 (m)
γ	–	–	–	1.34 (q, 7.2)	7.45–7.52 (m)	–	–	1.42 (tq, 7.5)
δ	–	–	–	0.88 (*t*, 7.2)	7.45–7.52 (m)	–	–	0.91 (*t*, 7.2)
γ–γ′	–	–	–	–	–	1.22–1.36 (bs)	–	–
δ′	–	–	–	–	–	0.87 (*t*, 6.9)	–	–

[a] Chemical shifts (δ) in ppm. $^nJ[^{117/119}Sn^1, H]^3$, $J(^1H, ^1H)$ in Hz are listed in square brackets and parenthesis, respectively.
[b] Multiplicity is given as s = singlet, d = doublet, dd = doublet of doublets, m = multiplet., q = quintet, bs = broad signal.
[c] See Fig. 3.47 for α, β, γ, δ, α′, β′, γ′, δ′.

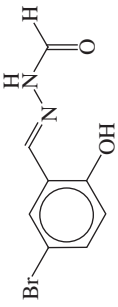

2.3.5. Diphenyltin(IV) [N′-(5-bromo-2-oxidobenzylidene)-N-(oxido methylene)hydrazine]; (4)

Compound **4** was prepared in the same way as **1**, using following quantities: N′-(5-bromo-2-hydroxybenzylidene)formohydrazide 0.73 g (3.0 mmol), diphenyltin(IV) dichloride 1.03 g (3.0 mmol), triethylamine 0.84 mL (6.0 mmol) were reacted in 1:1:2 ratio. Solid product was recrystallized in chloroform and *n*-hexane (4:1) mixture. IR (cm^{-1}): 1613 ν(C=N), 1073 ν(N–N), 570 ν(Sn–O), 469 ν(Sn–N).

*2.3.6. Dioctyltin(IV) [N′-(5-bromo-2-oxidobenzylidene)-N-(oxidom ethylene)hydrazine]; (**5**)*

Compound **5** was prepared in the same way as **1**, using following quantities: N′-(5-bromo-2-hydroxybenzylidene)formohydrazide 0.73 g (3.0 mmol), dioctyltin (IV)oxide 1.09 g (3.0 mmol) were reacted in 1:1 ratio. Viscous liquid product was obtained. IR (cm^{-1}): 1611 ν(C=N), 1082 ν(N–N), 569 ν(Sn–O), 460 ν(Sn–N).

2.3.7. Di-tert-butyltin(IV) [N′-(5-bromo-2-oxidobenzylidene)-N-(oxidomethylene)hydrazine]; (6)

Compound **6** was prepared in the same way as **1**, using following quantities: N′-(5-bromo-2-hydroxybenzylidene)formohydrazide 0.73 g (3.0 mmol), di-*tert*-butyltin(IV) dichloride 0.91 g (3.0 mmol), triethylamine 0.84 mL (6.0 mmol) were reacted in 1:1:2 ratio. Solid product was recrystallized in chloroform and *n*-hexane (4:1) mixture. IR (cm^{-1}): 1614 ν(C=N), 1088 ν(N–N), 564 ν(Sn–O), 465 ν(Sn–N).

*2.3.8. Butyltin(IV) [N -(5-bromo-2-oxidobenzylidene)-N-(oxidomet hylene)hydrazine] chloride; (**7**)*

Compound **7** was prepared in the same way as **1**, using following quantities: N′-(5-bromo-2-hydroxybenzylidene)formohydrazide 0.73 g (3.0 mmol), butyltin(IV) chloridedihydroxide 0.74 g (3.0 mmol) were reacted in 1:1 ratio. Solid product was recrystallized in chloroform and *n*-hexane (4:1) mixture (Scheme 1c). IR (cm^{-1}): 1608 ν(C=N), 1080 ν(N–N), 560 ν(Sn–O), 468 ν(Sn–N).

3. Results and discussion

3.1. Spectroscopy

In IR spectra of the ligand, the vibration bands due to νN–H, νO–H and νC = O were observed at 3185, 3410 and 1706 cm^{-1}, respectively. Due to enolization and deprotonation of the ligand on complexation with diorganotin moiety, the νC = O band vanished. The shifting of νC = N band at 1609 cm^{-1} to lower energy suggests the coordination of azomethine nitrogen to the Sn atom [23]. The shifting of N–N band from 1098 cm^{-1} by a value of ~20 cm^{-1} on complexation can be attributed to the decrease in repulsion of the lone pairs of electrons on the nitrogen atoms [24]. The presence of new bands associated with νSn–O and νSn–N, that were absent in the precursors, further indicates the formation of complexes [25].

In ^{1}H NMR chemical shift assignments of the diorganotin(IV) moiety are straightforward from the multiplicity pattern and/or resonance intensities; whereas the ligand skeleton was assigned by multiplicity patterns and/or resonance intensities (Table 1). In the spectra of ligand, single resonance is observed at 5.11 ppm, which is absent in the spectra of all complexes, indicating the substitution of phenolic proton by organotin moiety. The coordination of azomethine nitrogen with Sn atom shifted the CH=N proton resonance signal down field by a value of ~0.3 ppm with ^3J (^{119}Sn, ^{1}H) coupling constant value in the range 37–48 Hz.

The CSnC angle calculated for compound **1** from ^2J (^{119}Sn, ^{1}H) value, using Lockhart's equation $\{\theta = 0.0105\,[^2J]^2 - 0.799\,[^2J] + 122.4\}$, is 126° (Table 3) thus, confirming five-coordinate geometry around

Table 2
^{13}C NMR data of N′-(5-bromo-2-hydroxybenzylidene)formohydrazide (H_2L)[a,b] and its organotin(IV) derivatives.

Carbon		Chemical Shift (ppm)						
		H_2L	(1) Me_2SnL	(2) Et_2SnL	(3) n-Bu_2SnL	(4) Ph_2SnL	(5) Oct_2SnL	(6) ter-Bu_2SnL	(7) BuClSnL
−CH=N−		141.1	161.5	161.5	161.4	161.6	161.3	161.0	162.8
−N=CHO−		165.5	165.5	166.3	166.1	166.3	166.3	167.1	165.4
		156.0, 133.8, 128.4, 121.7, 118.9, 111.0	164.1, 138.1, 135.7, 123.8, 117.6, 108.2	164.4, 138.0, 135.7, 123.7, 117.6, 107.8	164.3, 138.0, 135.7, 123.7, 117.7, 107.8	164.2, 138.2, 135.9, 124.1, 117.7, 108.6	164.3, 138.0, 135.6, 123.7, 117.8, 107.8	164.4, 137.8, 135.5, 123.8, 117.7, 107.4	165.0, 137.0, 135.9, 124.5, 118.9, 108.3
R	α	–	1.6 [646, 618]	14.6 [609, 578]	22.5 [596, 571]	138.4 [639, 609]	22.9 [595, 568]	45.0 [566, 540]	25.6 [615, 595]
	β	–	–	9.4 [42]	27.0 [36]	136.1 [56, 55]	24.6 [36]	29.5	28.3 [38]
	γ	–	–	–	26.5 [89]	129.0 [89]	–	–	27.3 [87]
	δ	–	–	–	13.6 [20]	130.9 [17]	–	–	14.1 [19]
	γ−γ′	–	–	–	–	–	33.4 [82], 29.1, 29.0, 31.8, 22.6	–	–
	δ′	–	–	–	–	–	14.5	–	–
^{119}Sn		–	−162.8	−201.1	−200.7	−342.2	−201.0	−291.6	−200.1

[a] Chemical shifts (δ) in ppm. $^{n}J[^{117/119}Sn\ ^{13}C]$, $^{n}J[^{119}Sn,\ ^{13}C]$ in Hz are listed in parenthesis.
[b] See Fig. 3.47 for α, β, γ, δ, α', β', γ', δ'.

Table 3
(C−Sn−C) angles (°) based on NMR parameters of selected of complexes **1-7**.

Comp. No	Compound	$^{1}J(^{119}Sn,\ ^{13}C)$ (Hz)	$^{2}J(^{119}Sn,\ ^{1}H)$ (Hz)	Angle(°)	
1	Me_2SnL	646	79	133.4	129.6
2	Et_2SnL	609	–	130.2	–
3	n-Bu_2SnL	596	–	134.5	–
4	Ph_2SnL	639	–	138.5	–
5	Oct_2SnL	595	–	134.4	–
6	t-Bu_2SnL	566	–	131.7	–
7	BuClSnL	615	–	136.3	–

Sn atom. The characteristic signals for all the magnetically non-equivalent alkyl- or phenyl-protons of the organotin moieties have also been assigned, which are in good agreement with reported values [26].

The characteristic resonance peaks in ^{13}C NMR spectra of the complexes were recorded in $CDCl_3$, Table 2. The ^{13}C NMR spectra of the complexes show a considerable up field shift of all carbon resonances, compared with the ligand acid. This may be a consequence of an electron density shift from the ligand to the acceptor. In organotin compounds, the ^{1}J [^{119}Sn, ^{13}C] value is an important parameter to assess the coordination number of the Sn atom. The calculated coupling constants for compounds **1-7** were found to be in the range 566–646 Hz, which described the penta-coordinate environment about the Sn atom in these compounds [27].

The presence of a single ^{119}Sn peak for complexes **1-7** (Table 2) is in conformity with the formation of a single species having penta-coordinated Sn atom [28].

3.2. X-ray structure of H_2L

Crystal data and structure refinements of ligand H_2L are given in Table 4. Selected bond angles and distances are listed in Table 5. Fig. 1 shows the molecular structure along with atomic numbering

Table 4
Crystal data and structure refinement parameters for ligand H_2L

Compound No.	H_2L
Empirical formula	$C_8H_7BrN_2O_2$
Formula mass	243.07
Crystal system	Monoclinic
Space group	$P\ 2_1/c$
a(Å)	3.827(3)
b(Å)	24.259(2)
c(Å)	9.441(8)
α(°)	90.00
β(°)	100.48(4)
γ(°)	90.00
V(Å^3)	861.9(12)
Z	4
Crystal habit	Block
size (mm)	0.49 × 0.43 × 0.39
ρ (g.cm^{-3})	1.873
μ (Mo K_α) (mm^{-1})	4.73
F(000)	480
Total reflections	2527
Independent reflections	1859
For ($F_o \geq 4.0\sigma(F_o)$)	1420
$R(F) = \sum(\|\|F_o\| - \|F_c\|\|)/\sum\|F_o\|$	0.033
For (F_0>4.0 σ(F_0))	
$wR(F^2) = [\sum[w(F_o^2 - F_c^2)^2]/\sum[w(F_o^2)^2]]^{1/2}$	0.053
Goodness-of-fit	1.203
θ Range (deg)	2.35–30.10
Data/restrictions/params	1859/0/140
Largest diff. peak and hole (eÅ^{-3})	−0.82 and 1.18

Table 5
Selected bond lengths (Å) and bond angles (°) of ligand H_2L.

Bond lengths			
N(1)–C(7)	1.275 (6)	O(1)–C(6)	1.348 (6)
N(1)–N(2)	1.377 (6)	O(2)–C(8)	1.227 (7)
N(2)–C(8)	1.323 (7)	Br(1a)–C(3)	1.896 (5)
Bond angles			
C(2)–C(3)–Br(1a)	120.37 (4)	N(1)–C(7)–C(1)	120.95 (4)
C(4)–C(3)–Br(1a)	119.34 (4)	O(2)–C(8)–N(2)	123.67 (5)
O(1)–C(6)–C(5)	117.52 (4)	C(7)–N(1)–N(2)	116.68 (4)
O(1)–C(6)–C(1)	123.14 (4)	C(8)–N(2)–N(1)	118.33 (4)

Table 6
Hydrogen-bond geometry (Å, °) for ligand H_2L^e.

D–H···A	D–H	H···A	D···A	D–H···A
O(1)–H(1)···N(1)	0.81	1.84	2.649(3)	136
N(2)–H(2)···O(2)	0.77	2.10	2.866(2)	171

scheme. It contains nearly a planar salicylaldimine fragment which is benzenoid like as shown by most of the azomethines. The molecule forms both an intramolecular hydrogen bond, O(1)–(H1)…N(1) 2.649(3) and intermolecular hydrogen bond, N(2)–H(2)…O(2) 2.866 Å; the O(1)H(1)N(1) angle is 136° (Table 6). The N(1)–C(7) and O(2)–C(8) bond length (1.275(6), 1.227(7) Å) indicates double bond character. However, the N(1)–N(2), N(2)–C(8) and O(1)–C(6) bond lengths (1.377(6), 1.323(7) and 1.348(6) Å) are in close agreement with the single bond values reported in literature [29]. The original formyl group is retained in the crystal structure and is at *trans* position to the phenolic hydroxyl group. The data pertaining to inter and intra-molecular hydrogen bonds is provided in Table 6.

3.3. X-ray structure of 1 and 4

The asymmetric unit of **1** contains two different molecules; a stereoview of the molecules and atomic numbering scheme are shown in Fig. 2, while crystal data and selected bond lengths and bond angles are given in Tables 7 and 8, respectively. The structure of complex **1** consists of a deprotonated ONO dibasic tridentate ligand bonded to the $(CH_3)_2Sn(IV)$ moiety via two oxygen and a nitrogen atom, forming a O_2NC_2 core around the Sn atom. The ligand is non-planar, probably due to the steric requirements of the five and six membered chelate rings formed. The τ value is an important parameter to decide the geometry of five-coordinated metal and can be calculated by using equation $\tau = (\beta\text{-}\alpha)/60$ [30], where β and α are the consecutive largest of the basal angles around the Sn atom. For five-coordinated Sn with a perfect trigonal-bipyramidal geometry τ value is one whereas a value of zero corresponds to a perfect square-pyramidal structure. The two molecules have a bit different geometry as clear from τ value, (0.5 and 0.37). The τ value 0.5 for molecules one indicates a geometry midway between trigonal bipyramidal and square-pyramidal while distorted square-pyramidal geometry can be assigned to the second molecule. The different geometry of molecule 2 from that of molecule 1 may be due to less crowding of Sn center as evident from large $H_3C–Sn–CH_3$ angle (155.19°). The methyl group are further away from one another providing enough room for oxygen atom of the adjacent molecule to interact with Sn atom (Fig. 3). Thus, the two enolic oxygens are at the apical positions and the two methyl carbons and azomethinic nitrogen in the equatorial positions. The $Sn–O_{shorter}$ (2.106 and 2.086 Å) and Sn–O longer bond lengths (2.145 and 2.166 Å) are less than the sum of van der Waal's radii of Sn and O (2.8 Å). The O–Sn–N (equatorial) and O–Sn–O (axial) angles also show a large deviation from the ideal values thus, confirming highly distorted trigonal bipyramidal geometry. The Sn–N bond distances of the two molecules are closer to the sum of covalent radii of Sn and N (2.15 Å) and significantly less than the sum of van der Waal's radii (3.75 Å), as shown in Tables 8 and 9. The packing diagram of **1** (Fig. 3) confirmed secondary NCH–N, Sn–O, π–H and O–H interactions, resulting in a supramolecular cage structure.

Crystal data and selected interatomic parameters for compound **4** are collected in Tables 10 and 11, respectively. An ORTEP view of the molecule **4** including numbering scheme is shown in Fig. 4. The Sn is coordinated to the carbon of two phenyl groups and a tridentate ligand that is bonded to the Sn via a phenolic oxygen O(1), azomethine nitrogen N(1) and amide oxygen O(2). For compound **4**, the geometry around Sn is a midway between trigonal bipyramidal and square-pyramidal as evident from the τ value, 0.5. The equatorially positions are occupied by the nitrogen atom and two *ipso*-carbon of the phenyl groups; the two oxygen atoms are present at the apical position. The angle of O(1)Sn(1)O(2) is 157.29(14)°. Sn(1) atom form a six membered ring with O(1), C(1), C(6), C(7), N(1) atoms, while the Sn(1) atom forms a five membered ring with O(2), C(8), N(2) and N(1) atoms. The Sn–O(1) and Sn–O(2) bond lengths (2.068(3) and 2.140(3) Å) are less than the sum of Van der Waals radii of Sn and O (2.8 Å). The low values of O(1)–Sn–N(1), and O(2)–Sn–N(1) angles are 84.32° and 73.04°, respectively, and are significantly different to those expected for a regular geometry. The Sn–N(1) bond distance, 2.160 Å, is comparable to the sum of covalent radii of Sn and N (2.15 Å) and has considerably lower value than the sum of Van der Waals radii (3.75 Å) of the two atoms suggesting a strong tin-nitrogen bond. The C(1)–O(1) and C(8)–O(2) bond length (1.313 Å, 1.274 Å) are in agreement with the reported values [31].

The packing diagram (Fig. 5) indicates a dimeric structure for compounds **4** in which the two molecules are linked together via non-covalent secondary Br–Br intermolecular interactions with a distance of 3.589 Å. The intramolecular hydrogen bond, H–Br,

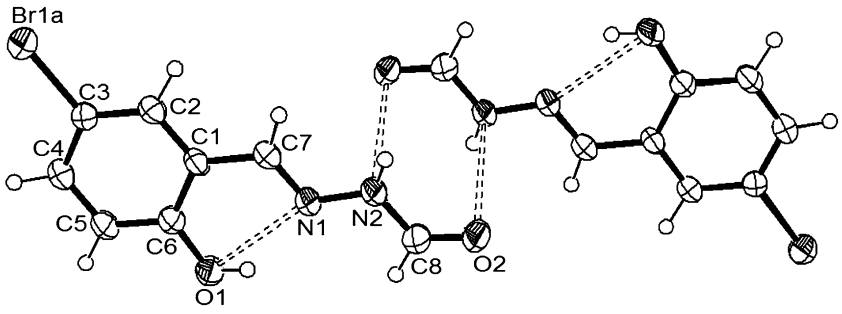

Fig. 1. ORTEP drawing of H_2L^e with the atomic numbering scheme. The dashed line indicates hydrogen bonds.

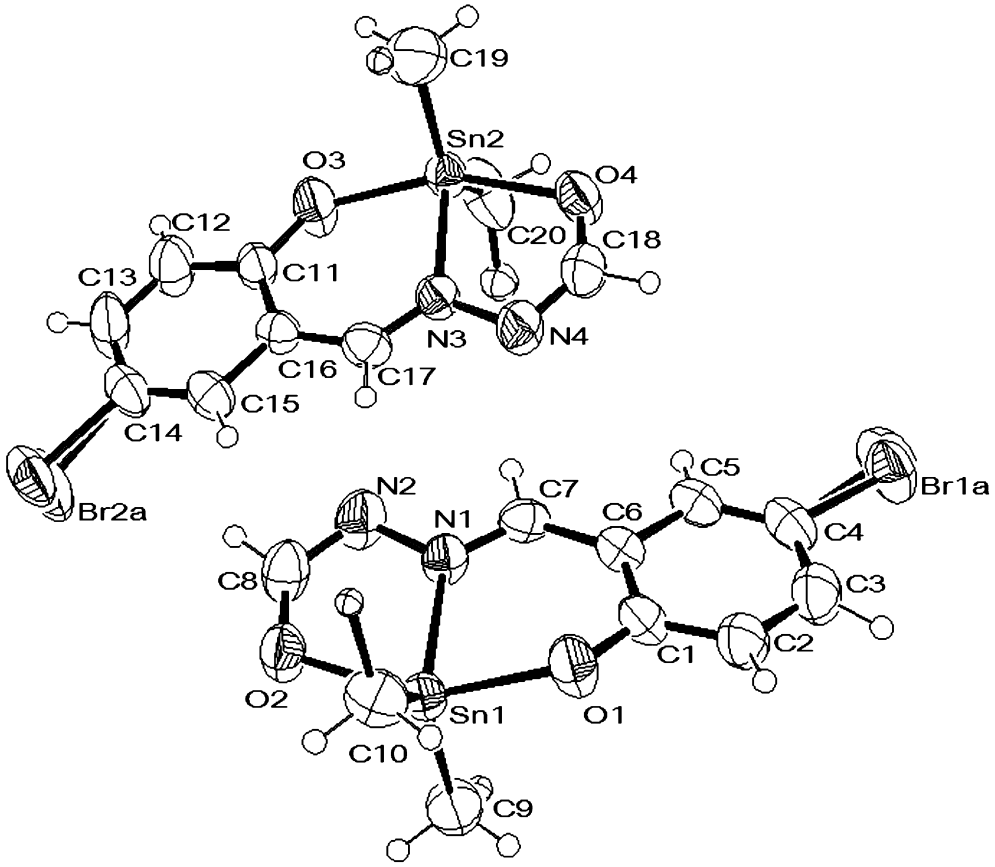

Fig. 2. ORTEP drawing of complex 1 with the atomic numbering scheme.

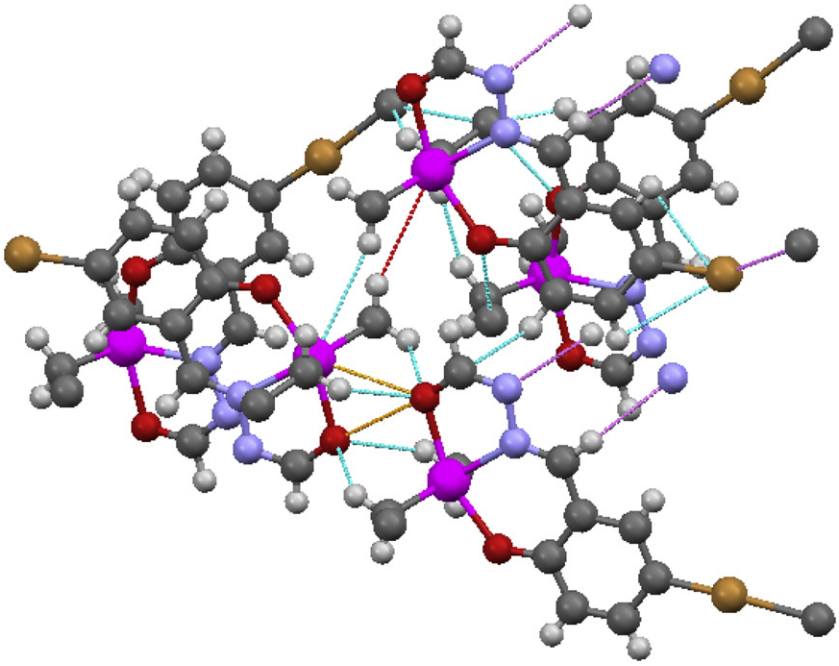

Fig. 3. Supramolecular cage structure of for one of the two molecules of compound **1** showing intermolecular Sn—O interactions.

Table 7
Crystal data and structure refinement parameters for compounds **1.**

Empirical formula	$C_{10}H_{11}BrN_2O_2Sn$
Formula mass	425.26
Crystal system	Monoclinic
Space group	$P\,2_1/c$
a (Å)	11.4406(5)
b (Å)	15.6641(6)
c (Å)	14.4624(7)
α(°)	90.00
β(°)	98.39(2)
γ(°)	90.00
V (Å^3)	2563.9(2)
Z	4
Crystal habit	Block
size (mm)	0.449 × 0.40 × 0.38
T (K)	296 (2)
ρ (g.cm^{-3})	1.102
μ (Mo K_α) (mm^{-1})	2.654
F(000)	812
Total reflections	7059
Independent reflections	4723
For ($F_o \geq 4.0\sigma(F_o)$)	
$R(F) = \sum(\|\|F_o\| - \|F_c\|\|)/\sum\|F_o\|$	0.048
For F_0>4.0 σ(F_0)	
$wR(F^2) = [\sum[w(F_o^2 - F_c^2)^2]/\sum[w(F_o^2)^2]]^{1/2}$	0.127
Goodness-of-fit	1.138
θ Range (deg)	1.93–30.54
Data/restrictions/params	4723/0/361

exits in both molecules, however, the bond value is not exactly the same (2.954 and 2.758 Å); the difference of about 0.196 Å is there.

4. Biological activities

4.1. Antifungal activity

The antifungal activity of synthesized compounds was tested *in vitro* against human pathogenic fungal strains including yeasts (*Candida albicans* ATCC 2192, *Candida glabrata* ATCC 90030), dermatophytes (*Microsporum canis* ATCC 9865, *Trichphyton longifusus* ATCC 22397), opportunistic molds (*Aspergillus flavus* ATCC 1030 and *Fusarium solani* ATCC 11712) by using the agar tube dilution test. The parent ligand (H_2L) is inactive against all the studied strain except *M. canis* and *F. solani,* where the ligand has comparable activity to the standard drug, especially against the latter strain. In general **1**, **2** and **7** are the least active organotin derivatives. The activities of complexes 3–6 are fairly good, especially against *A. flavus* and *F. solani*. The strain *C. glabrata* is quite resistant to all complexes (Fig. 6).

Table 8
Bond distances (Å) and bond angles (°) for compound 1 (molecule 1).

Bond lengths			
Sn(1)–C(9)	2.089(8)	N(1)–C(7)	1.286(8)
Sn(1)–C(10)	2.095(5)	N(1)–N(2)	1.403(8)
Sn(1)–O(1)	2.106(5)	N(2)–C(8)	1.293(10)
Sn(1)–O(2)	2.145(5)	C(8)–O(2)	1.284(9)
Sn(1)–N(1)	2.205(5)	O(1)–C(1)	1.321(8)
O(2)–C(8)	1.284(9)		
Bond angles			
C(1)–O(1)–Sn(1)	130.13(4)	C(8)–O(2)–Sn(1)	114.18(5)
O(1)–C(1)–C(2)	118.82(6)	C(10)–Sn(1)–C(9)	132.92(3)
O(1)–C(1)–C(6)	122.90(6)	O(1)–Sn(1)–C(9)	97.46(3)
N(1)–C(7)–C(6)	126.11(6)	O(1)–Sn(1)–O(2)	152.28(2)
O(2)–C(8)–N(2)	126.84(7)	O(1)–Sn(1)–N(1)	81.50(19)
C(7)–N(1)–Sn(1)	127.85(4)	C(9)–Sn(1)–N(1)	105.15(3)
N(2)–N(1)–Sn(1)	115.52(4)	O(2)–Sn(1)–N(1)	72.59(19)
C(9)–Sn(1)–O(2)	98.65(3)	C(10)–Sn(1)–N(2)	121.90(3)

Table 9
Bond distances (Å) and bond angles (°) for compound 1 (molecule 2).

Bond lengths			
Sn(2)–O(3)	2.086(5)	C(17)–N(3)	1.285(9)
Sn(2)–C(20)	2.100(8)	C(18)–O(4)	1.270(10)
Sn(2)–C(19)	2.110(10)	C(18)–N(4)	1.277(10)
Sn(2)–O(4)	2.166(5)	N(3)–N(4)	1.418(8)
Sn(2)–N(3)	2.169(5)	O(3)–C(11)	1.327(8)
O(4)–C(18)	1.270(10)		
Bond angles			
O(3)–C(11)–C(12)	119.46(7)	C(18)–O(4)–Sn(2)	112.73(5)
O(3)–C(11)–C(16)	122.47(6)	O(3)–Sn(2)–C(20)	92.93(3)
N(3)–C(17)–C(16)	125.91(6)	O(3)–Sn(2)–C(19)	95.44(4)
O(4)–C(18)–N(4)	128.68(5)	O(3)–Sn(2)–O(4)	155.19(2)
C(17)–N(3)–N(4)	114.48(6)	O(3)–Sn(2)–N(3)	82.74(2)
C(17)–N(3)–Sn(2)	129.07(5)	C(20)–Sn(2)–C(19)	132.47(4)
N(4)–N(3)–Sn(2)	116.29(4)	C(20)–Sn(2)–O(4)	94.72(3)
C(18)–N(4)–N(3)	109.58(6)	C(20)–Sn(2)–N(3)	115.78(3)
O(4)–Sn(2)–N(3)	72.68(2)	C(19)–Sn(2)–O(4)	96.68(4)
C(11)–O(3)–Sn(2)	133.60(4)	C(19)–Sn(2)–N(3)	111.68(3)

4.2. Antibacterial activity

The schiff base ligand and its diorganotin(IV) derivatives were screened for their antibacterial activity against 2 gram-positive (*Bacillus subtilis, Staphylococcus aureus*) and 4 gram-negative bacteria (*Eschericha coli, Shigella flexenari, Pseudomonas aeruginosa, Salmonella typhi*) using Imipenem ($C_{12}H_{17}N_3O_4S$) is used as a standard drug for comparison (Fig. 7). Most of the diorganotin(IV) derivatives significantly inhibit gram-positive bacterial growth. This may be due to the ease of permeation of the complexes owing to the simplicity of the cell wall of these strains. The high bactericidal activity of organotin derivatives than the parent ligand is most probably due to the reduction in the polarity of the central Sn atom upon coordination with the ligand. Two main factors are responsible for this reduction in polarity; firstly because of the partial sharing of its positive charge with donor groups and secondly due to π-electrons delocalization within the whole chelating ring. As consequence, the lipophilic nature of the central Sn atom increases, which favors the permeation of the complexes through the lipid layer of the cell membrane [32].

Table 10
Crystal data and structure refinement parameters for compound (4).

Empirical formula	$C_{20}H_{15}BrN_2O_2Sn$
Formula mass	513.94
Crystal system	Monoclinic
Space group	$P\,2_1/c$
a (Å)	19.514(13)
b(Å)	10.917(7)
c(Å)	9.196(5)
α(°)	90.00
β(°)	95.44(2)
γ(°)	90.00
V(Å^3)	1950.1(2)
Z	4
Crystal habit	Block
size (mm)	0.49 × 0.43 × 0.39
ρ (g.cm^{-3})	1.750
μ (Mo K_α) (mm^{-1})	3.375
F(000)	1000
Total reflections	5915
Independent reflections	3012
For ($F_o \geq 4.0\sigma(F_o)$)	
$R(F) = \sum(\|\|F_o\| - \|F_c\|\|)/\sum\|F_o\|\|$	0.038
For ($F_o > 4.0\sigma(F_o)$)	
$wR(F^2) = [\sum[w(F_o^2 - F_c^2)^2]/\sum[w(F_o^2)^2]]^{1/2}$	0.095
Goodness-of-fit	1.022
θ Range (deg)	1.05–30.49
Data/restrictions/params	3012/12/234
Largest diff. peak and hole (eÅ^{-3})	−0.423 and 0.671

Table 11
Selected bond lengths (Å) and bond angles (°) of compound (4).

Bond lengths			
Sn(1)–O(1)	2.068(3)	N(1)–N(2)	1.401(5)
Sn(1)–C(15)	2.107(2)	N(2)–C(8)	1.284(7)
Sn(1)–C(9)	2.133(4)	O(1)–C(1)	1.313(4)
Sn(1)–O(2)	2.140(3)	O(2)–C(8)	1.274(7)
Sn(1)–N(1)	2.160(4)	N(1)–C(7)	1.290(5)
Bond angles			
C(1)–O(1)–Sn(1)	132.82(2)	C(8)–O(2)–Sn(1)	113.20(3)
O(1)–C(1)–C(2)	119.27(3)	O(1)–Sn(1)–C(15)	94.62(12)
O(1)–C(1)–C(6)	123.11(4)	O(1)–Sn(1)–C(9)	94.54(14)
N(1)–C(7)–C(6)	126.84(4)	O(1)–Sn(1)–O(2)	157.29(14)
O(2)–C(8)–N(2)	127.53(3)	O(1)–Sn(1)–N(1)	84.32(12)
C(10)–C(9)–Sn(1)	121.89(4)	C(15)–Sn(1)–C(9)	127.49(15)
C(14)–C(9)–Sn(1)	119.42(4)	C(15)–Sn(1)–O(2)	95.50(15)
C(16)–C(15)–Sn(1)	121.40(4)	C(15)–Sn(1)–N(1)	120.45(12)
C(20)–C(15)–Sn(1)	118.57(19)	C(9)–Sn(1)–O(2)	95.33(16)
C(7)–N(1)–Sn(1)	127.68(3)	C(9)–Sn(1)–N(1)	111.86(13)
N(2)–N(1)–Sn(1)	116.18(3)	O(2)–Sn(1)–N(1)	73.04(15)

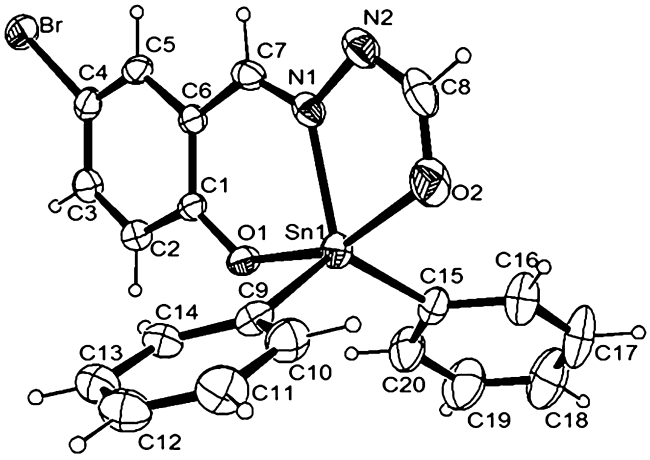

Fig. 4. ORTEP drawing of complex 4 with the atomic numbering scheme.

4.3. Anti-leishmanial activity

The Anti-leishmanial activity of ligand and complexes (**1**–**7**) was obtained against the pathogenic Leishmania major, using Amphotericin B (0.50 μg/mL) as standard drug (Table 12). The complexes (**1**–**7**) are more active than the parent ligand. The complexes activity decreases in the following order: **3 > 6 > 2 > 4 > 1 > 5 > 7**. The activity of the complexes **2**, **4** and **6** is as good as standard drug. The

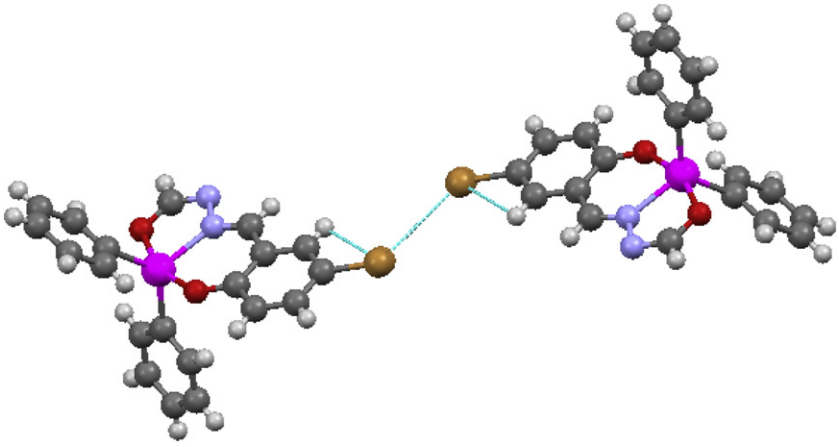

Fig. 5. Dimeric structure of compound **5** due to the presence of Br–Br interaction.

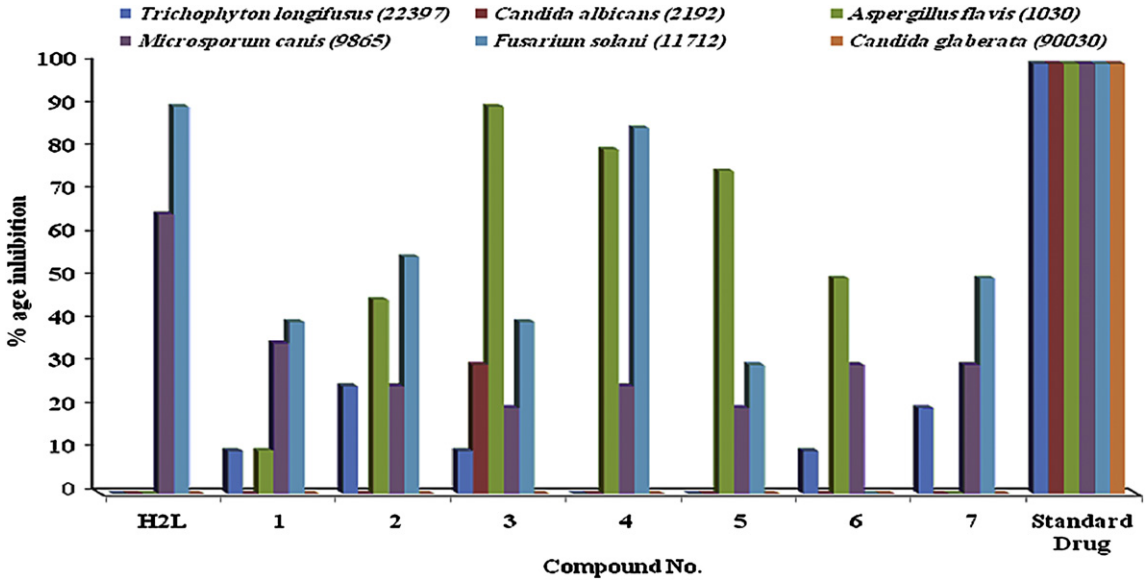

Fig. 6. Antifungal activity of H_2L^e and its organotin(IV) derivatives against various fungi.

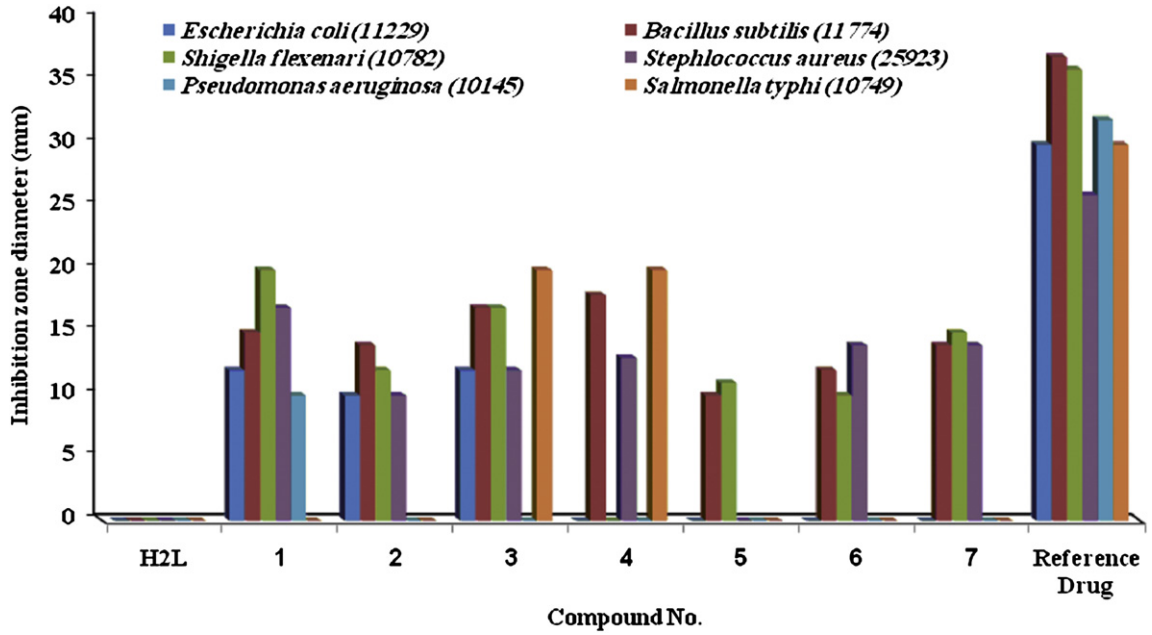

Fig. 7. Antibacterial activity[a,b] of N′-(5-bromo-2-hydroxybenzylidene)formohydrazide (H_2L^e) and its organotin(IV) complexes.

high activity of **3** and **6** than **2** can be explained on the basis their high lipophilic character. The low activity of *tert*-butyltin(IV) derivative (**6**) than *n*-butlyltin(IV) compound (**3**) may be due to reduce planarity of the former that slow down the complex diffusion. The high activity of **4** than **1** can be attributed to its planarity and lipophilicity. The low activity of **5** may be due to its high molecular weight that turn into reduction of its permeability. The lowest activity of the chlorobutyltin(IV) complex confirms the idea that monorganotins are least toxic than diorganotins [33]. The compound **3** inhibits the leishmanial growth even more effectively than Amphotericin B, and thus has a potential to be marketed as leishmanicidal agents.

Table 12
Antileishmanial activity[a–d] of selective ligands and their organotin(IV) complexes.

Compound No.	IC_{50} (μg/mL) ± S.D
H_2L^e	22.07 ± 0.33
(1)	4.28 ± 0.03
(2)	2.26 ± 0.02
(3)	0.41 ± 0.05
(4)	2.51 ± 0.01
(5)	5.21 ± 0.04
(6)	1.22 ± 0.02
(7)	8.11 ± 0.04

[a] Test organism: Leishmania major (DESTO).
[b] Standard drug: Amphotericin. B (μg/mL) ± S.D = 0.50 ± 0.02.
[c] Incubation period: 72 h.
[d] Incubation temperature: 22 ± 1 °C.

Table 13
Antiurease activity of representative ligands and their organotin(IV) complexes[a,b,c,d]

Compound No.	H_2L^e	(1)	(2)	(3)	(4)	(5)	(6)	(7)
% Inhibition	45.1	36.5	27.3	18.1	28.0	20.1	16.2	18.2
IC_{50} ± S.D [μM]	–	–	–	–	–	–	–	–

[a] Sample Concentration [mM] 0.5.
[b] Standard: Thiourea, IC_{50} ± SEM [μM], 21.0 ± 0.11.
[c] Proposed implications of inhibitor : Acute ulcer.
[d] IC_{50} reported for those compounds whose % inhibition is more than 55%.

4.4. Antiurease activity

Parent ligand and its complexes were tested for their *in vitro* urease inhibition activities at 0.5 mM concentration against jack bean urease. The urease inhibition activity was undertaken according to the literature protocols [34], using thiourea as the standard inhibitor having an IC_{50} value of 21 ± 0.01 μM. The results are presented in Table 13.The parent ligand and its organotin(IV) derivatives displayed moderate inhibition.

5. Conclusion

In summing up, seven new diorganotin(IV) compounds of [N′-(5-bromo-2-oxidobenzylidene)-N-(oxidomethylene)hydrazine have been synthesized and characterized by IR, NMR, mass spectroscopy and elemental analysis. The crystal structure of the parent ligand, dimethyl- and diphenyltin(IV) derivatives has also been determined by X-ray single crystal diffraction analyses. Both dimethyl- and diphenyltin(IV) derivatives have a distorted square-pyramidal (supramolecular structure) and a distorted trigonal-bipyramidal (dimeric structure) geometry, respectively. The synthesized complexes showed moderate antibacterial, antifungal and antiurease activities. Most of the complexes showed leishmanicidal activity comparable to those of standard drug. The highest activity was noted for complex **3** [IC_{50} (μg/mL) ± S.D = 0.41 ± 0.05], that exceeds the standard drug, the Amphotericin. B [IC_{50} (μg/mL) ± S.D = 0.50 ± 0.02] and may be used as a new metal-based leishmanicidal drug in future.

Acknowledgments

We thank the Higher Education Commission of Pakistan for financial support.

Appendix A. Supplementary data

CCDC 815286, 815288 and 815288 contains the supplementary crystallographic data for H_2Lcomplexes **1** and **4**, respectively. These

data can be obtained free of charge from The Cambridge Crystallographic Data Center via www.ccdc.cam.ac.uk/data_request/cif.

References

[1] R.H. Holm, J. Am. Chem. Soc. 82 (1960) 5632–5636.
[2] E.C. Niederhoffer, J.H. Timmons, A.E. Martell, Chem. Rev. 84 (1984) 137–203.
[3] K. Srinivasan, P. Michaud, J.K. Kochi, J. Am. Chem. Soc. 108 (1986) 2309–2320.
[4] W. Zhang, J.L. Loebach, S.R. Wilson, E.N. Jacobsen, J. Am. Chem. Soc. 112 (1990) 2801–2803.
[5] J. Tisato, F. Refosco, F. Bandoli, Coord. Chem. Rev. 135 (1994) 325–397.
[6] J. Lacroix, Eur. J. Inorg. Chem. 2 (2001) 339–348.
[7] J. Nagel, U. Oertel, P. Friedel, H. Komber, D. Mobius, Langmuir 13 (1997) 4693–4698.
[8] S.S. Sundari, A. Dhathathreyan, M. Kanthimathi, U.N. Balachandran, Langmuir 13 (1997) 4923–4925.
[9] H.L. Singh, A.K. Varshney, Appl. Organomet. Chem. 15 (9) (2001) 762–768.
[10] I. Omae, Appl. Organometal. Chem. 17 (2003) 81–105.
[11] M. Nath, S. Goyal, Met.-Based Drugs 2 (1995) 297–309.
[12] M. Nath, R. Yadav, M. Gielen, H. Dalil, D. de Vos, G. Eng, Appl. Organomet. Chem. 11 (1997) 727–736.
[13] R.S. Collinson, D.E. Ferton, Coord. Chem. Rev. 148 (1996) 19–40.
[14] A.K. Saxena, F. Huber, Coord. Chem. Rev. 95 (1989) 109–123.
[15] M. Gielen, A.G. Davies, K. Pannell, E. Tiekink, Tin Chemistry: Fundamentals, Frontiers, and Applications. Wiley, 2008.
[16] A.J. Crowe, P.J. Smith, C.J. Cardin, H.E. Parge, F.E. Smith, Cancer Lett. 24 (1984) 45–48.
[17] A.J. Crowe, P.J. Smith, J. Organomet. Chem. 244 (1982) 223–235.
[18] M. Gielen, E.R.T. Tiekink, Metallotherapeutic Drugs and Metal-Based Diagnostic Agents: The Use of Metals in Medicine. Wiley, 2005.
[19] A.J. Crowe, Drugs Future 12 (1987) 255–275.
[20] A.J. Crowe, P.J. Smith, G. Attasi, Chem. Biol. Interact 32 (1980) 171–178.
[21] B.B. Tushar, S.M. Cheerfulman, W. Willem, B. Monique, et al., J. Organomet. Chem. 690 (2005) 3080–3094.
[22] W.F.L. Armarego, C. Chai, Purification of Laboratory Chemicals, fifth ed. Butterworth, Oxford, 2003.
[23] H. Yin, J. Cui, Y. Qiao, Polyhedron 27 (2008) 2157–2166.
[24] M.A. Ali, A.H. Mirzam, A.L. Tan, L.K. Wei, P.V. Bernhardt, Polyhedron 23 (2004) 2037–2043.
[25] C. Pettinari, F. Marchetti, R. Pettinari, D. Martini, A. Drozodov, S. Troyanov, Inorg. Chim. Acta 325 (2001) 103–114.
[26] G.L. Sandhu, R. Hundal, E.R.T. Tiekink, J. Organomet. Chem. 430 (1992) 15–23.
[27] T.P. Lockhart, F. Davidson, Organometallics 6 (1987) 2471–2478.
[28] M. Nádvorník, J. Holeek, K. Handlí, A. Lyka, J. Organomet. Chem. 275 (1984) 43–51.
[29] F. Zhi, Y.-L. Yang, Acta Cryst E63 (2007) o4471.
[30] A.W. Addison, T.N. Rao, J. Reedijk, J. van Rijn, G.C. Verschoor, J. Chem. Soc. Dalton Trans. 7 (1984) 1349–1356.
[31] M.A. Affan, S.W. Foo, I. Jusoh, S. Hanapi, E.R.T. Tiekink, Inorganica Chim. Acta 362 (2009) 5031–5037.
[32] Zia-ur-Rehman, N. Muhammad, S. Shuja, S. Ali, I.S. Butler, A. Meetsma, M. Khan, Polyhedron 28 (2009) 3439–3448.
[33] M. Gielen, Appl. Organomet. Chem. 16 (2002) 481–494.
[34] M. Serwar, T. Akhtar, S. Hameed, K.M. Khan, Synthesis, urease inhibition and antimicrobial activities of some chiral 5-aryl-4-phenylpropyl-1,2,4-triazoles, Arkivoc vii (2009) 210–221.